Additive Schwarz Methods without Subdomain Overlap and with New Coarse Spaces

Petter E. Bjørstad [1] Maksymilian Dryja [2] Eero Vainikko [3]

1 Introduction

This chapter develops two additive Schwarz methods with new coarse spaces. The methods are designed for elliptic problems in 2 and 3 dimensions with discontinuous coefficients. The methods use no explicit overlap of the subdomains, subdomain interaction is via the coarse space. The first method has a rate of convergence proportional to $(H/h)^{1/2}$ when combined with a suitable Krylov space iteration. This rate is independent of discontinuities in the coefficients of the equation. The method has good parallelization properties and does not require a coarse grid triangulation, that is, one is free to use arbitrary, irregular subdomains. The second method uses a diagonal scaling in addition to the standard coarse space. This method is not as robust and flexible as the first method. A suitable model problem that we will consider has the variational form:

[1] Para//ab, Institutt for Informatikk, University of Bergen, N-5020 Bergen, Norway. http://www.ii.uib.no/~petter, Email: petter@ii.uib.no. This research was partially supported by NFR grant 27625.
[2] Department of Mathematics, Warsaw University, Banacha 2, 02-097 Warsaw, Poland. Email: dryja@mimuw.edu.pl. This research was partially supported by the NSF under grant NSF-CCR-9204255, and in part by the Colorado School of Mines.
[3] Para//ab, Institutt for Informatikk, University of Bergen, N-5020 Bergen, Norway.

Domain Decomposition Methods in Sciences and Engineering, edited by R. Glowinski *et al.*

Find $u^* \in V(\Omega)$ such that

$$\sum_{i=1}^{N} \int_{\Omega_i} \rho_i \nabla u^* \cdot \nabla v \, dx = \int_{\Omega} f v \, dx \quad \forall v \in V(\Omega), \tag{1}$$

in an appropriate Sobolev space $V(\Omega)$. Here ρ_i are positive constants and $\Omega = \cup_{i=1}^{N} \Omega_i$. We are interested in the discontinuous coefficient case, i.e., we have (possibly large) jumps in the values of ρ_i across subdomain boundaries.

This problem is quite common in practice where, for example, the coefficients ρ_i represent physical (e.g., material) properties that change across the domain of interest. An example of this is petroleum reservoir simulation [BK95], where the reservoir consists of inhomogeneous rock where the permeability can change by orders of magnitude across relatively small sections. The freedom to make the subdomain boundaries follow the material discontinuities may be quite important in this and similar applications.

The problem has attracted much attention, [Sko92] and [BS92] developed parallel algorithms showing experimentally that the Additive Schwarz algorithm converged very satisfactorily when using small or minimal overlap between the subdomains. The paper [BX91] contains estimates for the weighted L^2-projection indicating a lack of stability and in [Xu91] there are counter examples showing that these estimates are sharp. The report [DSW94] discusses many domain decomposition algorithms for this problem in 3 dimensions and characterizes a class of distributions of the coefficients ρ_i for which the L^2-projection is stable. This class, called a quasi-monotone distribution, requires a monotone path from all subdomains to the subdomain having the largest coefficient, traversing (through the faces) the subdomains that have a common node [4], see Figure 1. For more references the reader should consult the bibliographies given in the above mentioned papers.

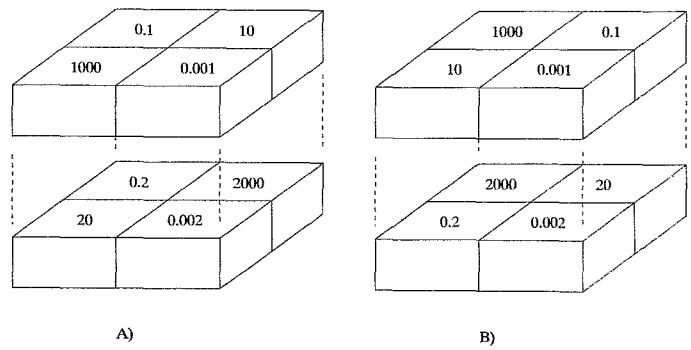

Figure 1 In A) the distribution is not quasi-monotone as there is no monotone path from 1000 to 2000. In B) we show a quasi-monotone distribution.

[4] If there is a path through edges only, we have a weak quasi-monotone distribution. This situation improves our estimates, but is not discussed further here.

2 Definition of a Discrete Model Problem

Let Ω be a polyhedral region in R^d, $d = 2, 3$. We consider two triangulations of Ω, a coarse and a fine, with elements Ω_i and e_i each having diameters H_i and h_i respectively. We assume that the fine triangulation is a refinement of the coarse subdivision. We further require a constant α_i, independent of the triangulation, such that

$$\hat{h}_i = \inf_{j:e_j \cap \partial\Omega_i} h_j \geq \alpha_i \sup_{j:e_j \cap \partial\Omega_i} h_j, \tag{2}$$

for each substructure Ω_i. This defines $\hat{h}_i$, the diameter of the smallest element touching the boundary in substructure Ω_i and requires the substructure boundary elements to be quasi-uniform. Note that elements in the interior of a substructure are not subject to this restriction, but we require all elements of the fine triangulation to be shape regular. We note that our assumptions can be relaxed to only require shape regularity near subdomain boundaries, at the expense of a more technical exposition. In order to keep the notation simple the reader should note that we often use the quantity h_i under the (limited) quasi-uniform assumption stated in (2).

We have no such assumption on the coarse triangulation, and note that our results are valid for an irregular coarse partitioning into subdomains as long as each element Ω_i with diameter H_i is a union of the fine triangles e_i. In order to keep the presentation simple we will only discuss the case where V^h is a finite element space of piecewise linear, continuous functions defined on the fine triangulation and vanishing on $\partial\Omega$, the boundary of Ω. Our discrete problem is of the form:

Find $u \in V^h(\Omega)$ such that

$$a(u, v) = f(v) \quad \forall v \in V^h(\Omega), \tag{3}$$

where

$$a(u, v) = \sum_{i=1}^{N} \int_{\Omega_i} \rho_i \nabla u \cdot \nabla v \, dx, \qquad f(v) = \int_{\Omega} fv \, dx \tag{4}$$

and ρ_i are positive constants.

3 The Additive Average Method

We decompose the space V^h into

$$V^h = V_0 + V_1 + \cdots + V_N,$$

where, for $i = 1, \cdots, N$, $V_i = H_0^1(\Omega_i) \cap V^h$ and zero outside of Ω_i. The space V_0, which we call the coarse space is defined as the range of an interpolation-like operator I_A, V_0 =Range(I_A). For $u \in V^h$ on $\bar{\Omega}_i$ we define $I_A u$ as follows:

$$I_A u = \begin{cases} u(x), & x \in \partial\Omega_{ih} \\ \bar{u}_i, & x \in \Omega_{ih}, \end{cases} \tag{5}$$

where $\partial\Omega_{ih}$ and Ω_{ih} denote the nodal points of $\partial\Omega_i$ and Ω_i respectively. Let n_i denote the number of nodes on $\partial\Omega_i$. For any function $u \in V^h$ we define the quantity $\bar{u}_i$ for

each $\partial\Omega_i$ by

$$\bar{u}_i = \frac{1}{n_i} \sum_{x \in \partial\Omega_{ih}} u(x), \tag{6}$$

the average of the nodal values of u that are on the boundary of substructure Ω_i. Due to this construction and in order to distinguish this method from other additive Schwarz methods, we will denote it the Additive Average method.

We now state a lemma about the properties of our interpolation-like operator I_A which will be useful for the analysis of the proposed algorithm.

Lemma 1. For any $u \in V^h$:

$$a(I_A u, I_A u) = \sum_i \rho_i |I_A u|^2_{H^1(\Omega_i)} \leq C \sum_i \rho_i \frac{H_i}{\hat{h}_i} |u|^2_{H^1(\Omega_i)} \tag{7}$$

and

$$\sum_i \rho_i ||u - I_A u||^2_{L^2(\Omega_i)} \leq C \sum_i \rho_i H_i^2 |u|^2_{H^1(\Omega_i)}, \tag{8}$$

where C is a constant independent of H_i and h_i and of the jumps in ρ_i. Here $\hat{h}_i$ is defined in (2).

Proof: First, consider the interpolation error $||u - I_A u||^2_{L^2(\Omega_i)}$. We have in d dimensions ($d = 2, 3$),

$$\begin{aligned} ||u - I_A u||^2_{L^2(\Omega_i)} &\leq 2 \left\{ ||u||^2_{L^2(\Omega_i)} + \int_{\Omega_i} (I_A u)^2 dx \right\} \\ &\leq C \left\{ ||u||^2_{L^2(\Omega_i)} + H_i^d \, \bar{u}_i^2 \right\}. \end{aligned} \tag{9}$$

We can estimate $\bar{u}_i^2$ by

$$\bar{u}_i^2 \leq C H_i^{1-d} ||u||^2_{L^2(\partial\Omega_i)},$$

since

$$\bar{u}_i^2 = \frac{1}{n_i^2} \Big(\sum_{x \in \partial\Omega_{ih}} u(x) \Big)^2 \leq \frac{1}{n_i} \sum_{x \in \partial\Omega_{ih}} u(x)^2 \tag{10}$$

and $1/n_i \leq C(h_i/H_i)^{d-1}$ because of assumption (2).

Using this, we obtain an intermediate inequality which is needed in the proof of both (7) and (8),

$$||u - I_A u||^2_{L^2(\Omega_i)} \leq C \left\{ ||u||^2_{L^2(\Omega_i)} + H_i ||u||^2_{L^2(\partial\Omega_i)} \right\}. \tag{11}$$

We now proceed to prove (7).

$$\begin{aligned} |I_A u|^2_{H^1(\Omega_i)} &= |I_A u - \bar{u}_i|^2_{H^1(\Omega_i)} \\ &\leq C \sum_{e_j \subset \bar{\Omega}_i} h_j^{-2} ||I_A u - \bar{u}_i||^2_{L^2(e_j)} \\ &\leq C h_i^{d-2} \sum_{x \in \partial\Omega_{ih}} (u(x) - \bar{u}_i)^2 \\ &\leq C h_i^{d-2} \sum_{x \in \partial\Omega_{ih}} u^2(x), \end{aligned}$$

where we have used the inverse inequality and the properties of I_A. The last inequality follows from the observation that,

$$\sum_{x\in\partial\Omega_{ih}} (u(x)-\bar{u_i})^2 = \sum_{x\in\partial\Omega_{ih}} (u(x)-\bar{u_i})u(x) = \sum_{x\in\partial\Omega_{ih}} (u^2(x)-n_i\bar{u_i}^2) \leq \sum_{x\in\partial\Omega_{ih}} u^2(x).$$

From this we conclude that

$$|I_A u|^2_{H^1(\Omega_i)} \leq \frac{C}{h_i}||u||^2_{L^2(\partial\Omega_i)}. \tag{12}$$

Using the trace inequality

$$||u||^2_{L^2(\partial\hat{\Omega})} \leq C\left\{|u|^2_{H^1(\hat{\Omega})} + ||u||^2_{L^2(\hat{\Omega})}\right\}, \tag{13}$$

for a reference element $\hat{\Omega}$, of unit diameter, see for example Theorem 1.5.1.10 in [Gri85], we can write:

$$\begin{aligned}
|I_A u|^2_{H^1(\Omega_i)} &\leq Ch_i^{-1}||u||^2_{L^2(\partial\Omega_i)} \\
&\leq Ch_i^{-1}H_i^{d-1}||u||^2_{L^2(\partial\hat{\Omega})} \\
&\leq Ch_i^{-1}H_i^{d-1}\left\{|u|^2_{H^1(\hat{\Omega})} + ||u||^2_{L^2(\hat{\Omega})}\right\} \\
&\leq Ch_i^{-1}H_i^{d-1}\left\{\frac{1}{H_i^{d-2}}|u|^2_{H^1(\Omega_i)} + \frac{1}{H_i^d}||u||^2_{L^2(\Omega_i)}\right\} \qquad (14) \\
&\leq C\frac{H_i}{\hat{h}_i}|u|^2_{H^1(\Omega_i)},
\end{aligned}$$

where we have used Poincare's inequality on the second term in the last step. Summation over all elements Ω_i proves (7), the first part of the lemma.

In order to prove the second part of Lemma 1, we apply the result from (14) to the second term of (11) and Poincare's inequality on the first term concluding that

$$||u - I_A u||^2_{L^2(\Omega_i)} \leq CH_i^2|u|^2_{H^1(\Omega_i)}.$$

Summation over all subdomains Ω_i completes the proof of Lemma 1.

Introduce bilinear forms $b_i(u,v)$ on $V_i \times V_i$ of the form

$$b_i(u,v) = a(u,v) \quad i = 1,\cdots,N$$

and the bilinear form on the coarse space

$$b_0(u,v) = \sum_i \rho_i \hat{h}_i^{d-2} \sum_{x\in\partial\Omega_{ih}} (u(x)-\bar{u_i})(v(x)-\bar{v_i}). \tag{15}$$

Note that for $v = \phi$, a basis function associated with a nodal point $x \in \partial\Omega_i$, we have

$$\sum_{x\in\partial\Omega_{ih}} (u(x)-\bar{u_i})(\phi(x)-\bar{\phi_i}) = \sum_{x\in\partial\Omega_{ih}} (u(x)-\bar{u_i})\phi(x),$$

since

$$\sum_{x\in\partial\Omega_{ih}} (u(x)-\bar{u}_i)\bar{\phi}_i = 0.$$

Let

$$T = T_0 + T_1 + \cdots + T_N, \tag{16}$$

where

$$b_i(T_i u, v) = a(u,v) \qquad \forall\, v \in V_i,\ \ i = 0,\cdots,N.$$

The discrete problem (3) can be replaced by the equation

$$Tu = g,$$

where $g = \sum_{i=0}^{N} g_i$, and $g_i = T_i u$ is the solution of

$$b_i(g_i, v) = f(v) \qquad \forall\, v \in V_i.$$

We refer the reader to [SBG95] for a detailed explanation of this reformulation.

We now state the main result of this paper:

Theorem 1 *The operator T is self-adjoint positive definite in V^h with the scalar product $a(u,v)$ and for any $u \in V^h$*

$$\gamma_0 \delta^{-1} a(u,u) \le a(Tu,u) \le \gamma_1 a(u,u),$$

where γ_0 and γ_1 are positive constants independent of h_i and H_i and of the jumps of ρ_i. Here $\delta = \max_i H_i/\hat{h}_i$ and $\hat{h}_i$ is defined in (2).

Proof: Using the general framework of Additive Schwarz methods (Chapter 5 in the book [SBG95]), we need to check three key assumptions.

Assumption 1 *Let C_0 be the minimum constant such that for all $u \in V^h$ there exists a representation $u = \sum_i u_i,\ \ u_i \in V_i$, with*

$$\sum_i b_i(u_i, u_i) \le C_0^2 a(u,u).$$

Let $u_0 = I_A u$ and $w = u - u_0$. Note that w vanishes on each $\partial\Omega_i$. In light of this let us define $u_i \in V_i$ by the nodal values of w at all nodal points $x \in \Omega_{ih}$ and zero otherwise. Note that

$$u = \sum_{i=0}^{N} u_i.$$

We then have

$$\begin{aligned}
\sum_{i=1}^{N} b_i(u_i,u_i) &= \sum_{i=1}^{N} \rho_i |u-u_0|^2_{H^1(\Omega_i)} \\
&= a(u-u_0, u-u_0) \\
&\le 2a(u,u) + 2a(u_0,u_0).
\end{aligned}$$

We now apply Lemma 1 to the second term above and obtain

$$\sum_{i=1}^{N} b_i(u_i, u_i) \leq C\delta a(u, u). \tag{17}$$

It remains to handle the case $i = 0$, that is, u_0. We use the same inequalities as in the proof of the first part of Lemma 1 to estimate $b_0(u_0, u_0)$,

$$b_0(u_0, u_0) = \sum_i \rho_i \hat{h}_i^{d-2} \sum_{x \in \partial\Omega_{ih}} (u(x) - \bar{u}_i)^2 \leq C \sum_i \frac{\rho_i}{\hat{h}_i} ||u||^2_{L^2(\partial\Omega_i)}. \tag{18}$$

The inequality in (14) provides a bound on $||u||^2_{L^2(\partial\Omega_i)}$,

$$b_0(u_0, u_0) \leq C \sum_i \rho_i \frac{H_i}{\hat{h}_i} |u|^2_{H^1(\Omega_i)} \leq C\delta a(u, u).$$

Combining (17) and the previous inequality gives a final bound on the energy of our decomposition of u

$$\sum_{i=0}^{N} b_i(u_i, u_i) \leq C\delta a(u, u),$$

which verifies Assumption 1.

Assumption 2 *Define $0 \leq \mathcal{E}_{ij} \leq 1$ to be the minimal values that satisfy*

$$|a(u_i, u_j)| \leq \mathcal{E}_{ij} [a(u_i, u_i)]^{1/2} [a(u_j, u_j)]^{1/2} \quad \forall u_i \in V_i,\ u_j \in V_j,\ i, j = 1, \ldots, N.$$

Define $\rho(\mathcal{E})$ to be the spectral radius of $\mathcal{E} = \{\mathcal{E}_{ij}\}$. Note that we do not include the subspace V_0.

In our case $\rho(\mathcal{E}) = 1$ since $\mathcal{E}_{ii} = 1$ and $\mathcal{E}_{ij} = 0$ when $i \neq j$.

Assumption 3 *Let $\omega > 0$ be the minimum constant such that*

$$a(u, u) \leq \omega b_i(u, u) \qquad \forall u \in V_i,\ \ i = 0, \cdots, N.$$

First, for $i = 1, 2, ..., N$, we can take $\omega = 1$ since $b_i(u, v) = a(u, v)$. To handle the case $i = 0$ we use the inverse inequality,

$$\begin{aligned} a(u_0, u_0) &= \sum_{i=1}^{N} \rho_i |u_0|^2_{H^1(\Omega_i)} \\ &= \sum_{i=1}^{N} \rho_i |u_0 - \bar{u}_i|^2_{H^1(\Omega_i)} \\ &\leq C \sum_{i=1}^{N} \rho_i \hat{h}_i^{d-2} \sum_{x \in \partial\Omega_{ih}} (u_0(x) - \bar{u}_i)^2 \\ &= C b_0(u_0, u_0), \end{aligned}$$

which shows that ω can be taken equal to C.

Note that in the case when $b_0(u, v)$ is the exact bilinear form, that is, if $b_0(u, v) = a(u, v)$ then $\omega = 1$ and we have $\gamma_1 = 2$ in the upper bound of Theorem 1.

4 An Additive Diagonal Scaling Method

This method is a modification of the method in the previous section. We decompose our domain into non-overlapping subdomains as before. We use the classical coarse space, i.e., piecewise linear elements defined on the substructures, but complement this by yet another decomposition derived from solving a diagonal problem along all interior interfaces. That is, we define a local problem for each node on the interior interfaces (corresponding to a local subdomain equal to the support of the nodal basis function). This is just a special diagonal scaling, hence the name of the method. For a quasi-monotone distribution of the ρ_i the estimate of the resulting condition number for the preconditioned system is of the same order as for the method in Section 3 while in the general (non quasi-monotone) case it is worse by a factor H/h in 3 dimensions. Our theory for this method requires the triangulation of each substructure Ω_i to be quasi-uniform with parameter h_i. We also note that the method requires the substructures to form a regular decomposition, hence it is potentially less versatile.

We proceed to describe and analyze this method using the same notation and framework as before. The decomposition of the space V^h is of the form

$$V^h = V_{-1} + V_0 + V_1 + \ldots + V_N.$$

Here V_i, for $i = 1, \ldots, N$, are the same as in Section 3. The coarse space $V_0 = V^H$, is a space of piecewise linear functions on the coarse triangulation which vanish on $\partial\Omega$ (we assume that the coarse triangulation with triangular elements is shape regular). The space V_{-1} is called a diagonal space and is the restriction of V^h to $\Gamma = \cup_i \partial\Omega_i$. Functions in this space vanish at all nodal points outside Γ.

The bilinear form $b_i(u, v) : V_i \times V_i \to R$, for $i = 0, 1, \ldots, N$, is given by

$$b_i(u, v) = a(u, v) \quad u, v \in V_i,$$

while for $i = -1$

$$b_{-1}(u, v) = \sum_{i=1}^{N} \rho_i h_i^{d-2} \sum_{x \in \partial\Omega_{ih}} u(x)v(x). \tag{19}$$

The operators $T_i : V^h \to V_i$, $i = -1, 0, \ldots, N$, are defined by the bilinear forms above and

$$T = T_{-1} + T_0 + \cdots + T_N.$$

Theorem 2 *The operator T is self-adjoint positive definite in V^h with the scalar product $a(u, v)$ and for any $u \in V^h$*

$$\gamma_2 \delta^{-1} a(u, u) \leq a(Tu, u) \leq \gamma_3 a(u, u),$$

where

$$\delta = \max_i \begin{cases} \frac{H_i}{h_i}, & \Omega \subset R^d, d = 2, 3 \text{ when } \rho_i \text{ is quasi} - \text{monotone} \\ \frac{H_i}{h_i} \log \frac{H_i}{h_i}, & \Omega \subset R^2 \text{ when } \rho_i \text{ is not quasi} - \text{monotone} \\ (\frac{H_i}{h_i})^2, & \Omega \subset R^3 \text{ when } \rho_i \text{ is not quasi} - \text{monotone}, \end{cases}$$

and γ_2 and γ_3 are positive constants independent of h_i and H_i and of the jumps of ρ_i.

Proof:

We need to check the same three assumptions as in Section 3.

Assumption 1:

Let $u_0 = Q_H^\rho u$ be the L_2- projection with weights ρ_i from V^h on $V_0 = V^H$, that is,

$$\sum_{i=1}^{N} \rho_i (u_0, v)_{L^2(\Omega_i)} = \sum_{i=1}^{N} \rho_i (u, v)_{L^2(\Omega_i)} \quad \forall v \in V^H.$$

It is known that

$$\sum_{i=1}^{N} \rho_i ||u - u_0||^2_{L^2(\Omega_i)} \leq C \sum_{i=1}^{N} \rho_i H_i^2 |u|^2_{H^1(\Omega_i)}, \tag{20}$$

in the case when ρ_i has a quasi-monotone distribution, see [DSW94], while

$$\sum_{i=1}^{N} \rho_i ||u - u_0||^2_{L^2(\Omega_i)} \leq \begin{cases} C \sum_{i=1}^{N} \rho_i H_i^2 \log \frac{H_i}{h_i} |u|^2_{H^1(\Omega_i)}, & \Omega \subset R^2 \\ C \sum_{i=1}^{N} \rho_i H_i^2 \frac{H_i}{h_i} |u|^2_{H^1(\Omega_i)}, & \Omega \subset R^3, \end{cases} \tag{21}$$

in the general case, see [BX91] and [Xu91].

Let $w = u - u_0$ and on each Ω_i we define

$$w = w_I + w_B,$$

where $w_I(x) = w$ for all $x \in \Omega_{ih}$ and zero on $\partial\Omega_i$. Note that $w_B \in V_{-1}$. Let $u_i = w_I$ on Ω_i and zero outside of Ω_i, for $i = 1, 2, \ldots, N$, and $u_{-1} = w_B$. We see immediately that $u = \sum_{i=-1}^{N} u_i$.

Again using (14) we obtain,

$$\begin{aligned} h_i^{d-2} \sum_{x \in \partial\Omega_{ih}} u_{-1}^2(x) &\leq C h_i^{-1} ||u - u_0||^2_{L^2(\partial\Omega_i)} \\ &\leq C \frac{H_i}{h_i} \left\{ |u - u_0|^2_{H^1(\Omega_i)} + H_i^{-2} ||u - u_0||^2_{L^2(\Omega_i)} \right\}. \end{aligned} \tag{22}$$

We now sum over substructures applying (20) or (21) (depending on the distribution of the ρ_i) to the last term. The projection $u_0 = Q_H^\rho$ is L_2 and H^1 stable in the case of quasi-monotone coefficients ρ_i, otherwise the extra factor $\log(H_i/h_i)$ or H_i/h_i from (21) appears. Hence, with δ defined in Theorem 2,

$$b_{-1}(u_{-1}, u_{-1}) \leq C\delta a(u, u). \tag{23}$$

Using the same arguments we prove that

$$b_0(u_0, u_0) \leq C\delta^{1/2} a(u, u). \tag{24}$$

We now consider the estimates for $i = 1, \ldots, N$. We have

$$b_i(u_i, u_i) = b_i(w_I, w_I) \leq 2b_i(w, w) + 2b_i(w_B, w_B).$$

By using the inverse inequality and (22) we estimate the last term as follows:

$$b_i(w_B, w_B) \leq C h_i^{d-2} \sum_{x \in \partial\Omega_{ih}} \rho_i (u - u_0)^2(x) \leq C \rho_i \frac{H_i}{h_i} ||u - u_0||^2_{H^1(\Omega_i)}.$$

Hence,

$$\sum_{i=1}^{N} b_i(u_i, u_i) \leq C(\delta^{1/2} a(u,u) + a(w_B, w_B)) \leq C\delta a(u,u). \tag{25}$$

Adding (23), (24), and (25) we obtain

$$\sum_{i=-1}^{N} b_i(u_i, u_i) \leq C\delta a(u,u),$$

which verifies Assumption 1.

Assumption 2:

Note that we can take V_{-1} and V_0 as the coarse spaces. In this case $\rho(\mathcal{E}) = 1$ as in Section 3. This slightly modifies the standard theory regarding Assumption 3, as we get 2ω instead of ω, see [SBG95] for details.

Assumption 3:

This assumption is verified by noting that we have $\omega = 1$ for $i = 0, 1, \ldots N$, while $\omega \leq C$ for the case $i = -1$. In this case we use the same arguments as in the proof of Theorem 1.

5 Implementation

In this section we briefly discuss implementation of the Additive Average method, in particular the issues relevant for a parallel implementation.

The subdomain solution can proceed completely in parallel, consider therefore the coarse problem,

$$\begin{pmatrix} A_a & A_{ab} \\ A_{ab}^T & A_b \end{pmatrix} \begin{pmatrix} u_a \\ u_b \end{pmatrix} = \begin{pmatrix} 0 \\ v_b \end{pmatrix}. \tag{26}$$

We note that one extra unknown per subdomain, corresponding to the average values $\bar{u}_i$ from (6), has been introduced in the vector u_a. The vector u_b has one component for each node on all subdomain boundaries. The subscripts a and b denote average and boundary respectively. The linear system has a very special structure that can be exploited in the solution algorithm. First, from (15) we note that each block in the coarse matrix will contain a diagonal scaling of the form $\hat{h}_i^{d-2}\rho_i$. The block A_a is diagonal with entries n_i (ignoring the scaling), the number of nodes belonging to each substructure boundary. Similarly, the block A_{ab} contains the nonzero entry, -1, in such a way that the first block equation just expresses the relation (6) between average and boundary values. The block A_b is also diagonal and its values correspond to the number of subdomains that share a given node on the substructure boundaries.

Additive algorithms normally proceed by restricting the current vector to the coarse space, perform a coarse space solution and interpolate this solution back to the fine

grid. In our case the restriction operator is implemented as follows. First, the values of all interior nodes in a substructure are added and the result is stored in the vector v_a. Next, we compute the right hand side vector v_b according to the formula

$$v_b := v_b - A_{ab}^T A_a^{-1} v_a. \tag{27}$$

This computation is the transpose of the interpolation-like operator defined in (5).

We solve the coarse matrix problem (26) by first forming the Schur complement

$$S = A_a - A_{ab} A_b^{-1} A_{ab}^T.$$

Due to the special structure of the blocks we can explicitly compute S quite easily or multiply S with a vector in an inner iterative procedure. We next solve the Schur complement system

$$S u_a = -A_{ab} A_b^{-1} v_b$$

and then compute the values of the internal boundary nodes u_b by

$$u_b = A_b^{-1}(v_b - A_{ab}^T u_a).$$

The resulting values u_a and u_b are then added to the solutions from the subdomains in the standard additive fashion. This outline shows how the special structure of our coarse problem results in an efficient implementation and an overall algorithm very suitable for parallel computation.

Table 1 Computational complexity of the preconditioning step in the Additive Average method compared with the Additive Schwarz method with minimal overlap

	2-dimensions		3-dimensions	
Task	Average	Additive	Average	Additive
Subdomain (size)	$(n-1)^2$	$(n+1)^2$	$(n-1)^3$	$(n+1)^3$
Coarse problem (size)	m^2	$(m-1)^2$	m^3	$(m-1)^3$
Transfers (flops)	$2(n-1)^2+20n$	$34(n+1)^2$	$2(n-1)^3+30n^2$	$126(n+1)^3$
Communication (words)	2	$8(n+1)$	2	$12(n+1)^2$
Communication (startups)	2	10	2	14

6 Complexity

We compare the complexity of the preconditioning step in one iteration of a Krylov subspace method when using the classical Additive Schwarz method and our new Additive Average method. We consider only Additive Schwarz with minimal overlap, that is, each subdomain extends a distance h into its neighbor making the total overlap area have width $2h$. We give the required number of operations per subdomain in a way which can be implemented on a parallel machine where each subdomain is mapped

to a (possibly virtual) processor. Additionally, a full Krylov step requires some vector operations and a residual calculation (a distributed matrix vector product), but this has the same cost in the two methods.

For simplicity, we consider the case where we have m^d subdomains each having n^d rectangular grid blocks in d dimensions ($d = 2, 3$). This means that we have $(n-1)^d$ interior nodal points in each subdomain. We ignore the (setup) cost of forming the Schur complement described in the previous section. Table 1 shows that each subdomain problem is slightly smaller since we have no overlap in the new method, while the coarse problem has dimension m^d, an increase from $(m-1)^d$ for the Additive Schwarz method. One should also note that each subdomain problem in the new methods have a constant coefficient ρ_i, while in the Additive Schwarz method there are jumps in the coefficients near the subdomain boundaries because of the overlap. This may make the subdomain problems easier to solve with our new approach. The two coarse problems have similar nonzero structure. A potentially more significant difference can be seen in the reduced cost of performing the interpolation and restriction (called 'transfer' in Table 1) as well as the reduced communication requirement. The term $2(n-1)^2$ reflects the need to add all interior unknown values and later add the computed average value to all interior nodes, altogether two additions per nodal point. The term $20n$ estimates the work along the boundary of each subdomain according to the equations in the previous section and similarly $30n^2$ in 3 dimensions. The reduced communication reflects the fact that only one average value must be communicated (both ways) between the coarse solver and each subdomain. The Additive Schwarz algorithm has two phases of communication of similar size; after the subdomain solution and in the residual calculation. In the Additive Average method the first phase is very small and a full iteration of a parallel code will therefore have both the number of messages and the size of the messages reduced by almost 50 percent. We will describe actual parallel performance in a forthcoming report.

7 Numerical Results

We have carried out numerical experiments comparing the new Additive Average method and the Additive Diagonal Scaling method with the standard Additive Schwarz method. In all tests we consider both a quasi-monotone distribution and a distribution which is not quasi-monotone. The domain and the distributions are derived from Figure 1 by translation of the upper half in two dimensions, while the full 3-dimensional piece is translated in order to build the 3-dimensional examples. That is, the value of ρ is constant in each subdomain. The algorithms have been implemented as described, for convenience we use an (accurate) iterative solver for subdomain and coarse grid problems. We further used the constant 1.7 instead of h^{d-2} in (15) and (19) when $d = 2$ since this value produced slightly better results.

First consider Table 2. We compare the two distributions and a reference case where $\rho_i = 1$ in two dimensions. Note the distinct jump in the condition number for the Additive Diagonal Scaling method in the non quasi-monotone case, while the Additive Average method shows no such dependence. We note that the Additive Schwarz method works well for all cases, with a very low condition number for the quasi-monotone case considered in this example. The factor H/h changes by a factor 2

in the two parts of the table. We observe that both the Additive Average method and the Additive Diagonal Scaling method reflect this while the Additive Schwarz method only displays a clear H/h dependence in the non quasi-monotone case.

Table 2 Comparison of the methods in 2 dimensions. The number of iterations required to reduce the residual by 10^{-6} and a condition number estimate is listed.

	4×4 Subdomains, 4×4 Blocks			8×8 Subdomains, 8×8 Blocks		
Method	Average	Diagonal	Additive	Average	Diagonal	Additive
Overlap	0	0	2	0	0	2
$\rho = 1$	22 (11.2)	17 (6.41)	15 (5.34)	34 (25.4)	27 (13.4)	18 (7.64)
q-mon.	25 (11.6)	19 (6.71)	16 (4.68)	37 (25.8)	29 (13.7)	15 (4.64)
Not q-mon.	24 (11.7)	28 (18.0)	16 (5.11)	42 (25.7)	58 (50.8)	21 (9.88)

Table 3 Comparison of the methods in 3 dimensions. The number of iterations required to reduce the residual by 10^{-6} and a condition number estimate is listed.

	4^3 Subdomains, 4^3 Blocks			8^3 Subdomains, 8^3 Blocks		
Method	Average	Diagonal	Additive	Average	Diagonal	Additive
Overlap	0	0	2	0	0	2
$\rho = 1$	19 (7.95)	16 (5.47)	19 (10.4)	32 (21.3)	27 (13.5)	26 (18.7)
q-mon.	23 (8.46)	20 (6.29)	21 (9.13)	37 (21.6)	33 (15.1)	24 (11.8)
Not q-mon.	23 (8.47)	34 (53.2)	23 (12.8)	39 (21.9)	134 (351)	44 (51.9)

Table 3 contains a similar comparison in the 3 dimensional case. We observe qualitatively the same effects. The condition number estimates grow somewhat faster than the factor of two change in H/h, but the reader should note that the problem changes in both Tables 2 and 3, that is, the number of coefficient jumps corresponds to the number of subdomains.

The substantial increase in the condition number from a quasi-monotone case to a non quasi-monotone distribution is not always followed by a similar increase in computational work. As an example, using the Additive Diagonal Scaling method with 4^3 subdomains and 8^3 blocks per subdomain, the condition number changes from 52.9 to 237, while the required number of iterations only increases from 53 to 60. If we exclude the two smallest eigenvalues and compute the resulting 'effective condition numbers', we get 32.3 and 38.0 respectively, thus explaining the small change in iteration count.

In the non quasi-monotone case we note that the Additive Schwarz method has a factor 4 increase in its condition number (when H/h changes by a factor 2), while it performs very well in the other cases. A standard estimate for the required number of iterations thus predicts that the computational effort may increase by as much as a factor of two which is indeed the case here. The Tables show that the particular distribution of coefficients may have a significant influence on the actual rate of convergence of two of the algorithms and this effect is in agreement with the theoretical predictions.

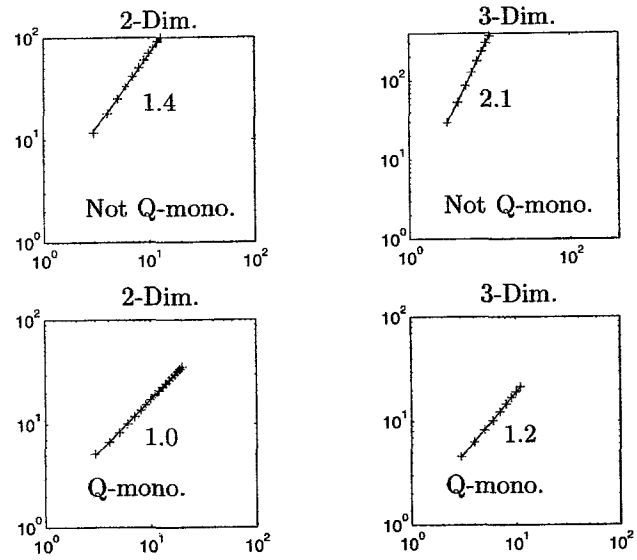

Figure 2 The Additive Diagonal Scaling method in 2 and 3 dimensions. The condition number of the iteration operator is plotted as a function of the ratio H/h. The least square fitted lines have slopes as indicated on the plots.

Figures 2 and 3 study the H/h behavior of the methods in more detail and compare this with the Additive Schwarz method in Figure 4. All computations are based on a domain subdivided into 4×4 subdomains in 2 dimensions and similarly into $4 \times 4 \times 4$ subdomains in 3 dimensions. We then change the ratio H/h by decreasing h. The log-log plots enable us to get an estimate for the slope β assuming that the condition number behaves like $(H/h)^{\beta}$. In Figure 2 we consider the Additive Diagonal Scaling method. The bottom part of the figure displays the quasi-monotone case and we observe a perfect slope of 1.0 in 2 dimensions, while the slope is near 1.2 in 3 dimensions. Both the actual condition numbers (crosses) and a line corresponding to a best least squares approximation are shown. In the non quasi-monotone case Theorem 2 predicts a slope near 2 in 3 dimensions and considerably better behavior in 2 dimensions, and we compute the values 2.1 and 1.4 respectively.

Figure 3 shows the same information for the Additive Average method. In this case there should be no sensitivity to the distributions and this is reflected fully in our computations. The slope is near 1.1 in 2 dimensions and near 1.2 in 3 dimensions. According to the theory presented the slopes should not exceed 1. The reason for this difference will be further investigated.

Finally, in Figure 4 we plot the behavior of the standard Additive Schwarz method with minimal overlap on the same test problems. In 2 dimensions our quasi-monotone problem converges with virtually no dependence on H/h. We therefore also include the case $\rho_i = 1$ (Poisson's equation) where the slope is about 0.7. The non quasi-monotone

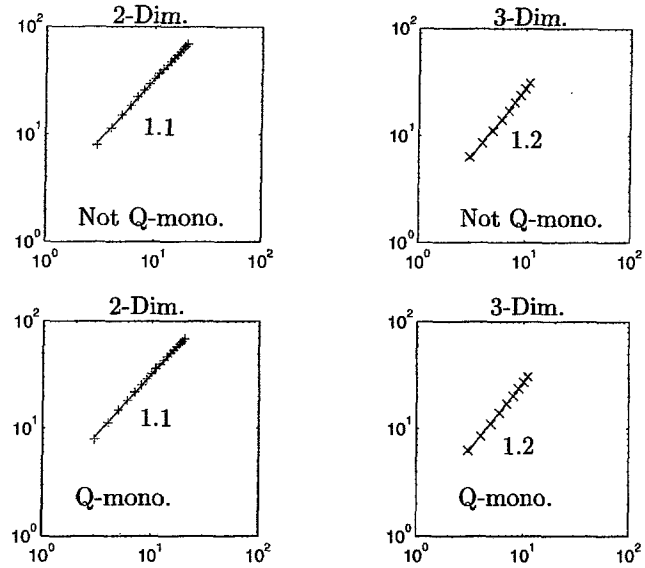

Figure 3 The Additive Average method in 2 and 3 dimensions. The condition number of the iteration operator is plotted as a function of the ratio H/h. The least square fitted lines have slopes as indicated on the plots.

case is also better than this having a slope of about 0.3. In 3 dimensions the overall picture looks similar, the non quasi-monotone case has a slope of 0.9, while the quasi-monotone distribution shows a slope of 0.3 (0.8 for a Poisson problem). This behavior is better than expected and different from the growth observed in Table 3. In that table the number of subdomains was allowed to grow (and therefore the number of jumps in the coefficients). The two cases are therefore not directly comparable, but a more detailed understanding of the Additive Schwarz method in this context is needed.

8 Conclusion

We have presented and analyzed two additive Schwarz methods, the Additive Average method and the Additive Diagonal Scaling method and compared them with the standard Additive Schwarz method with minimum overlap. Both methods behave well and are easy to implement. The Additive Average method has more flexibility since no regularity of the division into subdomains is required. We can also prove a satisfactory bound on the condition number for this method. The bound does not depend on assumptions of a quasi-monotone distribution of the coefficients. An increase in the condition number like H/h is predicted and this is often acceptable since a scaled up problem tend to be divided into more subdomains (keeping the ratio H/h bounded) in order to run efficiently on a scalable parallel computer.

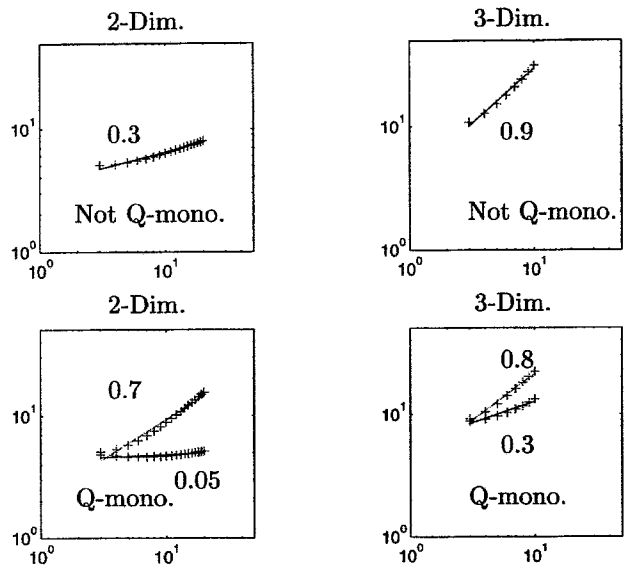

Figure 4 The Additive Schwarz method in 2 and 3 dimensions. The condition number of the iteration operator is plotted as a function of the ratio H/h. The least square fitted lines have slopes as indicated on the plots.

Our numerical experiments confirm the important difference that many methods exhibit when changing from a quasi-monotone to a non quasi-monotone distribution. Thus, this characterization of distributions where the weighted L^2 projection is stable is directly reflected in the behavior of some algorithms. However, it should be mentioned that a non quasi-monotone distribution is quite special. Both theory and computational experiments show that many methods are quite good even in the case where we only have a weak quasi-monotone distribution, that is, one can traverse through edges as well as faces in Figure 1. Additionally, there are cases where the growth in the condition number not necessarily implies a corresponding increase in the number of iterations.

The experiments further confirm that the Additive Average method is not affected by such a change in the distribution of the coefficients, but our estimates of the relevant condition number show a slightly faster growth with H/h than predicted by theory. The cause of this difference is at the present not fully determined and will be subject to further research.

Finally, it should be noted that the Additive Schwarz method shows better than predicted performance in both 2 and 3 dimensions on our test problems with discontinous coefficients. This observation has been reported earlier (see, for example [BS92]), but it is still not fully explained by theory.

References

[BK95] Bjørstad P. E. and Kårstad T. (1995) Domain decomposition, parallel computing and petroleum engineering. In Keyes D. E., Saad Y., and Truhlar D. G. (eds) *Domain-Based Parallelism and Problem Decomposition Methods in Computational Science and Engineering,* chapter 3, pages 39–56. SIAM.

[BS92] Bjørstad P. E. and Skogen M. (1992) Domain decomposition algorithms of Schwarz type, designed for massively parallel computers. In Keyes D. E., Chan T. F., Meurant G. A., Scroggs J. S., and Voigt R. G. (eds) *Fifth International Symposium on Domain Decomposition Methods for Partial Differential Equations,* pages 362–375. SIAM, Philadelphia, PA.

[BX91] Bramble J. H. and Xu J. (1991) Some estimates for a weighted L^2 projection. *Math. Comp.* 56: 463–476.

[DSW94] Dryja M., Sarkis M., and Widlund O. B. (March 1994) Multilevel Schwarz methods for elliptic problems with discontinuous coefficients in three dimensions. Technical Report 662, Department of Computer Science, Courant Institute. To appear in Numer. Math., 1995.

[Gri85] Grisvard P. (1985) *Elliptic Problems in Nonsmooth Domains.* Pitman, Boston.

[SBG95] Smith B. F., Bjørstad P., and Gropp W. (1995) *Domain Decomposition: Parallel Multilevel Methods for Elliptic Partial Differential Equations.* Cambridge University Press.

[Sko92] Skogen M. D. (February 1992) *Schwarz Methods and Parallelism.* PhD thesis, Department of Informatics, University of Bergen, Norway.

[Xu91] Xu J. (1991) Counter examples concerning a weighted L^2 projection. *Math. Comp.* 57: 563–568.